THE JOURNAL OF PHYSICAL CHEMISTRY A
A JOURNAL OF THE AMERICAN CHEMICAL SOCIETY

pubs.acs.org/JPCA

Article

Kinetics and Product Branching Ratio Study of the CH_3O_2 Self-Reaction in the Highly Instrumented Reactor for Atmospheric Chemistry

Published as part of The Journal of Physical Chemistry virtual special issue "Advances in Atmospheric Chemical and Physical Processes".

Lavinia Onel, Alexander Brennan, Freja F. Østerstrøm, Ellie Cooke, Lisa Whalley, Paul W. Seakins, and Dwayne E. Heard*

Cite This: *J. Phys. Chem. A* 2022, 126, 7639–7649

Read Online

ACCESS | Metrics & More | Article Recommendations | Supporting Information

ABSTRACT: The fluorescence assay by gas expansion (FAGE) method for the measurement of the methyl peroxy radical (CH_3O_2) using the conversion of CH_3O_2 into methoxy radicals (CH_3O) by excess NO, followed by the detection of CH_3O, has been used to study the kinetics of the self-reaction of CH_3O_2. Fourier transform infrared (FTIR) spectroscopy has been employed to determine the products methanol and formaldehyde of the self-reaction. The kinetics and product studies were performed in the Highly Instrumented Reactor for Atmospheric Chemistry (HIRAC) in the temperature range 268−344 K at 1000 mbar of air. The product measurements were used to determine the branching ratio of the reaction channel forming methoxy radicals, r_{CH3O}. A value of 0.34 ± 0.05 (errors at 2σ level) was determined for r_{CH3O} at 295 K. The temperature dependence of r_{CH3O} can be parametrized as $r_{CH3O} = 1/\{1 + [\exp(600 \pm 85)/T]/(3.9 \pm 1.1)\}$. An overall rate coefficient of the self-reaction of $(2.0 \pm 0.9) \times 10^{-13}$ cm^3 molecule^{-1} s^{-1} at 295 K was obtained by the kinetic analysis of the observed second-order decays of CH_3O_2. The temperature dependence of the overall rate coefficient can be characterized by $k_{overall} = (9.1 \pm 5.3) \times 10^{-14} \times \exp((252 \pm 174)/T)$ cm^3 molecule^{-1} s^{-1}. The found values of $k_{overall}$ in the range 268−344 K are ∼40% lower than the values calculated using the recommendations of the Jet Propulsion Laboratory and IUPAC, which are based on the previous studies, all of them utilizing time-resolved UV−absorption spectroscopy to monitor CH_3O_2. A modeling study using a complex chemical mechanism to describe the reaction system showed that unaccounted secondary chemistry involving Cl species increased the values of $k_{overall}$ in the previous studies using flash photolysis to initiate the chemistry. The overestimation of the $k_{overall}$ values by the kinetic studies using molecular modulation to generate CH_3O_2 can be rationalized by a combination of underestimated optical absorbance of CH_3O_2 and unaccounted CH_3O_2 losses to the walls of the reaction cells employed.

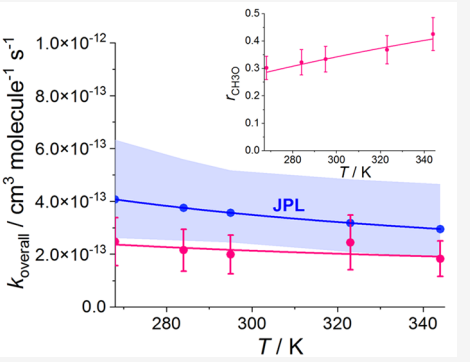

INTRODUCTION

Methyl peroxy (CH_3O_2) radicals are key species in atmospheric oxidation[1] and the combustion of volatile organic compounds.[2,3] The chemistry of CH_3O_2 in the troposphere is typically dominated by the reaction with NO, particularly in environments influenced by anthropogenic NO_x emissions (reaction R1). The reaction is a critical step in the tropospheric production of ozone in the presence of NO and converts NO into NO_2:

$$CH_3O_2 + NO \rightarrow CH_3O + NO_2 \quad (R1)$$

The subsequent reaction of CH_3O with O_2 produces HO_2, which then oxidizes another NO to NO_2:

$$CH_3O + O_2 \rightarrow CH_2O + HO_2 \quad (R2)$$

$$HO_2 + NO \rightarrow OH + NO_2 \quad (R3)$$

During the daytime the NO_2 photolysis is the dominant tropospheric source of O_3. In addition, the CH_3O_2 + NO reaction leads to the propagation of HO_x and NO_x radical chains. However, under low NO_x levels the self-reaction of CH_3O_2 and the reactions of CH_3O_2 with HO_2 and other organic peroxy (RO_2) species are significant losses of CH_3O_2

Received: July 13, 2022
Revised: September 13, 2022
Published: October 13, 2022

and terminate the radical chain. The CH_3O_2 self-reaction occurs through two channels, reactions R4.a and R4.b:[4]

$$CH_3O_2 + CH_3O_2 \rightarrow CH_3OH + CH_2O + O_2 \quad (R4.a)$$

$$CH_3O_2 + CH_3O_2 \rightarrow CH_3O + CH_3O + O_2 \quad (R4.b)$$

The methoxy radicals generated by channel R4.b subsequently react with oxygen (reaction R2) to form CH_2O and HO_2.

Despite its importance, the reported values for the rate coefficient of reaction R4, k_4, at room temperature lie in a wide range from $(2.7-5.2) \times 10^{-13}$ cm^3 molecule^{-1} s^{-1},[5] with IUPAC[5] and the Jet Propulsion Laboratory (JPL)[6] giving 20−40% and 40−50%, respectively, uncertainties at the 2σ level for k_4 in the temperature range 270−350 K. The previous kinetic studies used either the flash photolysis (FP) technique[7−11] or the molecular modulation (MM) method[12−14] to generate CH_3O_2 radicals, which were coupled to time-resolved UV−absorption spectroscopy to detect CH_3O_2 at fixed wavelengths in the range ∼210−270 nm (typically at 250 nm). As UV-absorption is a relatively insensitive technique, the detection limits of CH_3O_2 were high, for example around 4×10^{12} molecules cm^{-3},[8,11] and the UV-absorption studies used high initial concentrations of CH_3O_2, $10^{13}-10^{14}$ molecules cm^{-3} orders of magnitude.[7−11]

The kinetic studies of the CH_3O_2 self-reaction used photolytic mixtures of $CH_4/Cl_2/O_2$ to generate CH_3O_2.[7−14] CH_3O formed by the reaction R4.b is rapidly removed via the reaction with O_2 (reaction R2) in high concentrations ($10^{17}-10^{18}$ molecules cm^{-3} orders of magnitude)[7−14] to generate HO_2, which quickly reacts further with another CH_3O_2 radical (reaction R5).

$$CH_3O_2 + HO_2 \rightarrow CH_3OOH + O_2 \quad (R5)$$

As each HO_2 radical consumes rapidly one CH_3O_2 species on the time scale of the CH_3O_2 self-reaction, the determination of the overall rate coefficient of the reaction R4, k_4, requires knowledge of the branching ratios for reaction R4 (eq 1)[7,11]

$$k_{obs} = k_4(1 + r_{CH3O}) \quad (1)$$

where k_{obs} is the second-order observed rate coefficient and r_{CH3O} is the branching ratio of the reaction channel producing CH_3O (reaction R4.b).

The branching ratios in the CH_3O_2 self-reaction were the subject of a number of experimental studies performed from the mid 1970s to 1990 inclusive, which were followed by the study of Tyndall et al. in 1998.[15] The studies used photolysis of $CH_4/Cl_2/O_2$ or $(CH_3)_2N_2/O_2$ and either end product detection employing mass spectrometry (MS),[16] GC-MS,[17] and infrared spectroscopy,[15,18−20] or kinetic measurements using time-resolved UV−absorption spectroscopy.[7]

Some of the early studies reported a third channel of the self-reaction leading to CH_3OOCH_3 (reaction R4.c) with an insignificant contribution to the overall reaction rate coefficient at all temperatures—such as ≤0.08 at 297 K[19] and ≤0.07 at 298 K[18]—with other studies finding no evidence for any contribution of peroxide formation.[15,20]

$$CH_3O_2 + CH_3O_2 \rightarrow CH_3OOCH_3 + O_2 \quad (R4.c)$$

IUPAC[5] and JPL[6] use the evaluation of Tyndall et al.[21] that recommends considering reactions R4.a and R4.b as the sole reaction channels of the self-reaction.

The majority of the branching ratios studies were carried out at room temperature[15,16,18−20] and resulted in a range of values for the branching ratio of the reaction channel leading to CH_3O (reaction R4.b): r_{CH3O} = 0.22−0.45. Tyndall et al.[21] revised the room temperature results to obtain $r_{CH3O} = 0.37 \pm 0.06$ at 298 K, which is recommended by IUPAC[5] and JPL[6]. There have been two experimental studies of the temperature dependence of the branching ratios, which were conducted over different temperature ranges.[7,20] Lightfoot et al.[7] found a positive temperature dependence for r_{CH3O} between 388 and 573 K using flash photolysis in combination with time-resolved UV−absorption spectroscopy. Horie et al.[20] performed the only branching ratio experimental study covering temperatures below room temperature using matrix isolation Fourier transform infrared spectroscopy. The results were obtained from 223−333 K to show a positive temperature dependence for r_{CH3O}. Tyndall et al.[21] combined the results of Lightfoot et al.[7] and Horie et al.[20] with their recommended value at 298 K, $r_{CH3O} = 0.37 \pm 0.06$, and results published prior to 1990 to describe the ratio of the rate coefficients of the two reaction channels R4.a and R4.b as $\frac{k_{4.b}}{k_{4.a}} = (26.2 \pm 6.6) \times \exp[-(1130 \pm 240)/T]$. The evaluation of Tyndall et al.[21] is recommended by JPL.[6]

This work reports on the determination of the branching ratios and the overall rate coefficient of the CH_3O_2 self-reaction in the temperature range of 268−344 K at 1000 mbar of synthetic air. The kinetic and branching ratio measurements were performed in the Highly Instrumented Reactor for Atmospheric Chemistry (HIRAC). Fourier Transform Infrared (FTIR) spectroscopy was employed to monitor the time profiles of the concentrations of CH_2O and CH_3OH produced by the CH_3O_2 self-reaction to determine the branching ratios of the two reaction channels R4.a and R4.b.

The fluorescence assay by gas expansion (FAGE) method for the selective and sensitive detection of CH_3O_2 radicals was used to study the kinetics of the self-reaction.[22,23] The method involves the titration of CH_3O_2 to CH_3O by reaction with added NO, followed by the detection of the resultant CH_3O by off-resonant LIF with laser excitation at *ca.* 298 nm.[22] The FAGE instrument was calibrated for CH_3O_2 using the 184.9 nm photolysis of water vapor in air to generate OH followed by the conversion of OH to known concentrations of CH_3O_2 by reaction with CH_4 and O_2.[22,23] The 184.9 nm photolysis of water vapor is a well-established method of FAGE calibration for OH and HO_2.[24−26] The FAGE method for the CH_3O_2 detection has been validated previously using the direct and absolute near-IR Cavity Ring Down Spectroscopy (CRDS) method to detect CH_3O_2.[23]

FAGE measurements were carried out in the HIRAC chamber to determine the observed rate coefficient of the CH_3O_2 self-reaction, k_{obs}, at 1000 mbar and temperatures in the range of 268−344 K. Using k_{obs} and the branching ratio of the reaction channel leading to methoxy radicals, r_{CH3O}, the overall rate coefficient of the self-reaction, k_4, was derived. This is the first kinetic study of the CH_3O_2 self-reaction using a different detection method to that of UV−absorption spectroscopy.

EXPERIMENTAL SECTION

CH_3O_2 Generation in HIRAC. The HIRAC chamber is a stainless steel cylinder with an internal volume of ∼2.25 m^3 and has been described in detail elsewhere.[22,23,27,28] Four circulation fans mounted in pairs at each end of HIRAC are used to homogenize the gas mixture contained in the chamber.

https://doi.org/10.1021/acs.jpca.2c04968
J. Phys. Chem. A 2022, 126, 7639−7649

The photochemistry is initiated by eight UV lamps, each of them housed in a quartz tube. The quartz tubes are mounted radially inside the chamber (aligned parallel to the chamber longitudinal axis). In order to perform experiments at temperatures different to the room temperature a thermofluid (HUBE6479 DW-therm oil) is circulated from a high capacity thermoregulator (Huber Unistat 390W) through a series of stainless steel channels welded to the outside of the chamber. To ensure that the temperature is homogeneous within the chamber, the layout of these channels is evenly distributed on the chamber outer surface and HIRAC is lagged in a 20-mm-thick expanded neoprene.

The experiments were carried out at 268, 284, 295, 323, and 344 K and 1000 mbar of synthetic air obtained by mixing high purity oxygen (BOC, > 99.999%) and nitrogen (BOC, > 99.998%) in the ratio of O_2:N_2 = 1:4. CH_4 (BOC, CP grade, 99.5%) and Cl_2 (Sigma-Aldrich, ≥ 99.5%) were delivered to the chamber. Initial reagent concentrations in HIRAC were $[CH_4] = (2.0-3.0) \times 10^{17}$ molecules cm^{-3} and $[Cl_2] = (0.3-5.5) \times 10^{14}$ molecules cm^{-3}. After adding the reagents into the chamber, the lamps (Phillips, TL-D36W/BLB, λ = 350−400 nm) were turned on to generate CH_3O_2 by Cl_2 photolysis at ∼365 nm (reaction R6) followed by reactions R7 and R8. In the kinetic experiments the lamps were turned on for about 5 min, and then they were turned off to record the generated CH_3O_2 kinetic decay. In the experiments performed to determine the product branching ratio the lamps were turned on to measure CH_3OH and CH_2O using FTIR spectroscopy for a typical time of 20 min.

$$Cl_2 + h\nu(365nm) \rightarrow Cl + Cl \quad (R6)$$

$$CH_4 + Cl \rightarrow CH_3 + HCl \quad (R7)$$

$$CH_3 + O_2 + M \rightarrow CH_3O_2 + M \quad (R8)$$

Fourier Transform Infrared (FTIR) Measurements. An *in situ* multipass FTIR (Bruker IFS66) arrangement along the long axis of HIRAC was used to measure the concentrations of CH_2O and CH_3OH produced during the times with the lamps turned on. The multipass Chernin arrangement within the chamber was optimized for 72 internal reflections giving an approximate total path length of 128.5 m.[27,29] IR spectra were recorded every 30−60 s as the average of 30−100 scans at 1 cm^{-1} resolution. The concentration−time profiles for CH_2O and CH_3OH were obtained using the absorption at around 1740 cm^{-1} due to the stretch of the C═O bond of CH_2O and at around 1030 cm^{-1} due to the C−O stretch of CH_3OH and using reference spectra taken of formaldehyde and methanol. Reference spectra were taken delivering CH_2O and CH_3OH in known concentrations to the chamber under the same conditions as those used for the CH_3O_2 self-reaction experiments. The reference compound, either CH_2O or CH_3OH, was delivered in the vapor phase by direct heating of either liquid CH_3OH or *para*-formaldehyde powder in a glass finger connected to a one liter stainless steel cylinder to achieve a gas pressure of a few mbar. Then the gas was delivered from the cylinder to the chamber using a flow of N_2 (p_{N2} = 2000 mbar).

The reference spectra of CH_2O and CH_3OH were fitted to the observed IR absorbance recorded as a function of wavelength (λ) and time (t), $A_{obs_{\lambda,t}}$, between ∼1600−1900 cm^{-1} and ∼900−1120 cm^{-1}, respectively, at each time point to determine the changes to concentrations of CH_2O and CH_3OH vs time during the period of time with the lamps switched on (eq 2).

$$A_{obs_{\lambda,t}} = f_i A_{ref_{\lambda(i)}} \quad (2)$$

Here $A_{ref_{\lambda(i)}}$ is the reference IR absorbance of species i as a function of λ and $f_i = \frac{[i]_t}{[i]_{ref}}$, where $[i]_t$ is the concentration of species i at reaction time t and $[i]_{ref}$ is the concentration of species i giving the reference spectrum. The species i is CH_2O in the fit using $\lambda \cong$ 1600−1900 cm^{-1} and CH_3OH in the fit over ∼900−1120 cm^{-1}. The concentrations $[i]_t$ (i = CH_2O or CH_3OH) were then derived (eq 3).

$$[i]_t = f_i [i]_{ref} \quad (3)$$

FAGE Instrument and Calibration for CH_3O_2. Details on the HIRAC FAGE instrument are provided in previous publications.[22,23,30] The instrument sampled gas through a 1-mm-diameter pinhole mounted on one end of a 50-mm-i.d. flow tube at a rate of ∼3 slpm. The pressure inside the sampling tube was maintained at 3.3 mbar for a chamber pressure of 1000 mbar of synthetic air. A CH_3O fluorescence detection cell was integrated in the tube at ∼600 mm distance from the pinhole. About 25 mm prior to the detection cell, high purity NO (BOC, N2.5 nitric oxide) was injected at 2.5 sccm using a mass flow controller (Brooks 5850S) into the center of the gas flow to convert CH_3O_2 radicals into CH_3O. CH_3O radicals were subsequently detected by LIF spectroscopy, directing laser light at $\lambda_{online} \cong$ 297.79 nm to excite the $A^2A_1(\nu_3' = 3) \leftarrow X^2E(\nu_3'' = 0)$ transition of CH_3O with a 5 kHz pulse repetition frequency through the cell at a right angle to the gas flow. The off-resonant red-shifted LIF (320−430 nm) was monitored using photon counting. The laser background was measured at a wavelength of λ_{online} + 2.5 nm and then subtracted to obtain the fluorescence signal.

The FAGE technique requires calibration to convert the measured fluorescence signal into CH_3O_2 concentration. The calibration procedure has been described in detail previously[22,23] and hence only the important points are presented here. OH radicals were generated photolyzing water vapor in synthetic air at 184.9 nm to react with methane in excess (BOC, CP grade, 99.5%) to generate CH_3O_2. The produced air/radical mixture was then sampled by the FAGE instrument. The concentration of CH_3O_2 was determined using eq 4.

$$[CH_3O_2] = [OH] = [H_2O] \cdot \sigma \cdot \Phi \cdot F \cdot t \quad (4)$$

Here σ is the absorption cross section of water vapor at 184.9 nm, $(7.2 \pm 0.2) \times 10^{-20}$ cm^2 $molecule^{-1}$;[31,32] Φ is the photodissociation quantum yield of OH at 184.9 nm (unity), t is the photolysis time, and F is the lamp flux at 184.9 nm, which was varied to generate a range of CH_3O_2 radical concentrations. The product $F \times t$ was determined employing chemical actinometry.[28]

The FAGE calibration factor was utilized to determine $[CH_3O_2]$ in the HIRAC experiments:

$$[CH_3O_2] = \frac{S_{CH_3O_2}}{C_{CH_3O_2}} \quad (5)$$

where $S_{CH_3O_2}$ (counts s^{-1} mW^{-1}) is the recorded signal. Previous studies have shown that the FAGE sensitivity toward OH does not depend on the chamber temperature in the range 263−344 K,[33] and thus the calibration factor determined at a

https://doi.org/10.1021/acs.jpca.2c04968
J. Phys. Chem. A 2022, 126, 7639−7649

room temperature of 295 K, $C_{CH_3O_2}$ = (5.0 ± 1.7) × 10^{-10} counts cm^3 $molecule^{-1}$ s^{-1} mW^{-1}, was used in the kinetic analysis at all temperatures.

RESULTS

Product Branching Ratios in the CH_3O_2 Self-Reaction. To determine the branching ratios in the CH_3O_2 self-reaction (reactions R4.a and R4.b) the time profiles of the concentrations of the self-reaction products CH_3OH and CH_2O generated by turning the lamps on were recorded employing FTIR spectroscopy at a time intervals of 30−60 s. Over the first few minutes of the reaction [CH_3OH] and [CH_2O] increased linearly in time, showing that the removal of CH_3OH and CH_2O by secondary reactions is negligible. Figure S5 (Supporting Information) shows that at later reaction times [CH_3OH] vs time and [CH_2O] vs time curve down due to the secondary reactions of the products, predominantly the CH_3OH + Cl and CH_2O + Cl reactions. Numerical simulations carried out using a chemical mechanism described in the Supporting Information for the reaction system at 298 K show that, following about 25 s induction time, [CH_3OH] and [CH_2O] increase linearly during the first few minutes of the reaction (Figure S6).

Using the integrating rate ratio for the two parallel reactions R4.a and R4.b, eq 6 is obtained.

$$\frac{[CH_2O]_b}{[CH_3OH]} = \frac{2k_{4.b}}{k_{4.a}} \quad (6)$$

Here $[CH_2O]_b$ is the concentration of CH_2O formed by reaction R4.b followed by reaction R2. Taking into account that FTIR measures the sum of the concentrations of CH_2O produced by the two channels, i.e., $[CH_2O]_a$ produced by reaction R4.a and $[CH_2O]_b$ obtained by reactions R4.b + R2, and $[CH_2O]_a = [CH_3OH]$, eq 7 is derived from eq 6. Equation 7 was employed in previous FTIR product studies of the CH_3O_2 self−reaction.[15,19]

$$\frac{[CH_2O]_{overall}}{[CH_3OH]} = \frac{[CH_2O]_a + [CH_2O]_b}{[CH_3OH]} = \frac{k_{4.a} + 2k_{4.b}}{k_{4.a}} \quad (7)$$

Using eq 7 the branching ratio of the reaction channel R4.b, which produces CH_3O, is given by

$$r_{CH3O} = \frac{k_{4.b}}{k_{4.a} + k_{4.b}} = \frac{[CH_2O]_{overall} - [CH_3OH]}{[CH_2O]_{overall} + [CH_3OH]} \quad (8)$$

The branching ratio r_{CH3O} was determined using $[CH_2O]_{overall}$ and [CH_3OH] measured at early reaction times, when the product concentrations increased linearly in time (Figure S5 in the Supporting Information). A number (6−20) of values of r_{CH3O} were obtained at each temperature, 268, 284, 295, 323, and 344 K. Figure S7 (Supporting Information) shows that there was no trend with time in the extracted values over the initial few minutes used to determine r_{CH3O}, and thus the secondary reactions of CH_2O and CH_3OH can be neglected in the analysis.

The mean values of r_{CH3O} are shown in Figure 1 and Table S2 (Supporting Information). The results show a positive temperature dependence which can be characterized by r_{CH3O} = 1/{1 + [exp(600 ± 85)/T]/(3.9 ± 1.1)}, i.e., $k_{4.b}/k_{4.a}$ = (3.9 ± 1.1) × exp(−600 ± 85)/T. There have been two temperature dependence studies of the branching ratios previously, in the range 388−573 K[7] and between 223−333 K.[20] The result obtained by Horie et al.,[20] r_{CH3O} = 1/{1 + [exp(1131 ± 30/T)]/(19 ± 5)}, is shown in Figure 1, as the temperature range used by these authors overlaps with the range of temperatures where the measurements reported in the present work were carried out. In addition, Figure 1 shows r_{CH3O} derived from the evaluation of Tyndall et al.,[21] $k_{4.b}/k_{4.a}$ = (26.2 ± 6.6) × exp[−(1130 ± 240)/T], which is recommended by the Jet Propulsion Laboratory (JPL) evaluation.[6]

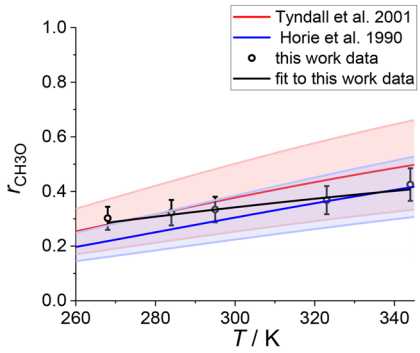

Figure 1. Product branching ratio for the channel giving CH_3O of the CH_3O_2 self-reaction, r_{CH3O}, as a function of temperature, T. The data obtained in this work are shown as open circles with the fit result, 1/{1 + [exp(600 ± 85)/T]/(3.9 ± 1.1)}, shown in black. The blue line and shading show the result of Horie et al.,[20] r_{CH3O} = 1/{1 + [exp(1131 ± 30/T)]/(19 ± 5)} and the red line and shading show r_{CH3O} vs T derived from $k_{4.b}/k_{4.a}$ vs T evaluated by Tyndall et al.,[21] (26.2 ± 6.6) × exp[−(1130 ± 240)/T] and recommended by the Jet Propulsion Laboratory evaluation.[6] All the errors are given at the 2σ level.

The values found by this work have overlapping error limits with the results reported by Horie et al.[20] and the values given by the recommendation of Tyndall et al.[21] at the 2σ level. However, the temperature dependence measured by Horie et al.[20] and the temperature dependence recommended by Tyndall et al.[21] are steeper than the increase in the value of r_{CH3O} with the temperature found in this study. The result at 295 K, $r_{CH3O(this\ work)}$ = 0.34 ± 0.05, is between the result of Horie et al.,[20] $r_{CH3O(Horie\ et\ al.)}$ = 0.29 ± 0.08, and the value recommended by Tyndall et al.,[21] $r_{CH3O(Tyndall\ at\ al.)}$ = 0.36 ± 0.12 (uncertainties at 2σ level).

The evaluation of Tyndall et al.[21] is based on the results of Horie et al.[20] between 223−333 K, Lightfoot et al.[7] in the range 388−573 K, results published prior to 1990 at $T \geq$ 373 K, and the result of the evaluation of the room temperature values, r_{CH3O}(298 K) = 0.37 ± 0.06.[15] The study of Horie et al.[20] is the single experimental study performed at temperatures in a range around room temperature, i.e., (293^{+40}_{-70}) K. The results of the present study agree well with the values reported by Horie et al.[20] at 323 and 344 K (Figure 1). However, going down in temperature $r_{CH3O(this\ work)}$ is increasingly higher than $r_{CH3O(Horie\ et\ al.)}$.[20]

Horie et al.[20] carried out flow tube experiments using photolysis of $CH_4/Cl_2/O_2$ mixtures to measure the ratio [CH_2O]/[CH_3OH], where CH_2O and CH_3OH were produced by the CH_3O_2 self-reaction, employing matrix isolation Fourier transform infrared spectroscopy. The authors performed numerical simulations based on a complex model to vary the rate coefficients of the self-reaction channels to match the measured values for [CH_2O]/[CH_3OH]. The authors

https://doi.org/10.1021/acs.jpca.2c04968
J. Phys. Chem. A 2022, 126, 7639−7649

found no evidence for the formation of CH_3OOCH_3 by the reaction channel R4.c. However, two sets of numerical simulations were performed: assuming a branching ratio of 0.1 for reaction R4.c and excluding reaction R4.c from the chemical mechanism used in the numerical simulations. Figure 1 shows the reported temperature dependence derived averaging the results generated by the two sets of simulations.[20] Considering a zero contribution for reaction R4.c, in line with the present recommendations,[5,6] the reported values of $r_{CH3O(Horie\ et\ al.)}$ increase by 5% over the temperature range 268−344 K and are lower than $r_{CH3O(this\ work)}$ by 7% at 295 K, 14% at 284 K, and 22% at 268 K.

The present work measured $[CH_2O]$ and $[CH_3OH]$ *in situ* to determine r_{CH3O} (eq 8), while Horie et al.[20] trapped the reaction products outside the reaction cell in a CO_2 matrix at 50 K to analyze them by IR spectroscopy to obtain $[CH_2O]/[CH_3OH]$, which was then used in the determination of r_{CH3O}. The concentrations of CH_2O produced by the self-reaction were corrected taking into account CH_2O formed in the matrix using a correction factor less than 10%. The lower values obtained for $r_{CH3O(Horie\ et\ al.)}$ relative to $r_{CH3O(this\ work)}$ at $T \leq 295$ K can be explained by a process leading to the CH_2O removal enhanced by reducing the reaction temperature which was not included in the reaction mechanism employed in the analysis performed by the authors.[20] Horie et al.[20] reported evidence of aerosol formation at 213 K resulting in unaccounted removal of CH_2O leading to a value of $[CH_2O]/[CH_3OH]$ lower than unity, a result which was not expected based on the reaction mechanism; the results obtained at 213 K were thus excluded from the analysis. The experiments below room temperature used in the determination of r_{CH3O}—i.e., in the range 223−298 K—were reported "free" of aerosols. However, $[CH_2O]$ and $[CH_3OH]$ in the experiments were relatively large, a few times higher than in the present work, increasing the potential of oligomers/particle formation at low temperatures.

Kinetics of the CH_3O_2 Self-Reaction. Figure 2 shows examples of CH_3O_2 decay generated by turning the HIRAC lamps off following the production of CH_3O_2 by the Cl atom initiated oxidation of CH_4 in the presence of O_2 (reactions R6 and R7) at 323 K. Kinetic decays were obtained in a similar fashion at all temperatures. The CH_3O_2 decays at each temperature, 268, 284, 295, 323, and 344 K, measured using FAGE were fitted simultaneously to the integrated second-order rate law equation describing the CH_3O_2 self-reaction (R4)):

$$\frac{1}{[CH_3O_2]_t} = \frac{1}{[CH_3O_2]_0} + 2k_{obs}t \quad (9)$$

where $[CH_3O_2]_t$ is the methyl peroxy concentration at reaction time t, $[CH_3O_2]_0$ is the initial concentration when the lights are switched off and k_{obs} is the observed rate coefficient. In line with previous analysis,[23] this work found that the loss of CH_3O_2 to the walls of HIRAC was negligible over the time scale of 0.5−1 min of the kinetic measurements at all temperatures employed, and hence a wall loss was not included in the kinetic analysis. Typically about 20 CH_3O_2 decays were fitted simultaneously at each temperature to obtain k_{obs} with the results shown in Table 1.

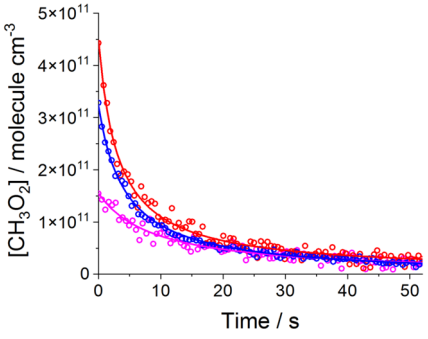

Figure 2. Examples of observations of CH_3O_2 (open circles) and fits to the data (solid lines) generated employing eq 9. The experiments used $Cl_2/CH_4/O_2$ and black lamps (see main text for details); 323 K and 1000 mbar mixture of N_2:O_2 = 4:1. At time zero the lamps were turned off. $[CH_4]_0 = 2.5 \times 10^{17}$ molecules cm^{-3} for all the kinetic decays. Initial Cl_2 concentrations: 3.3×10^{14} molecules cm^{-3} (red), 2.4×10^{14} molecules cm^{-3} (blue), and 7.5×10^{13} molecules cm^{-3} (magenta).

Table 1. Observed Rate Coefficient, k_{obs} for the CH_3O_2 Self-Reaction Measured in This Work

Temperature/K	k_{obs} (this work)[a]/cm^{3}molecule^{-1} s^{-1}
268	$(3.2 \pm 1.1) \times 10^{-13}$
284	$(2.9 \pm 1.0) \times 10^{-13}$
295	$(2.7 \pm 0.9) \times 10^{-13}$
323	$(3.4 \pm 1.4) \times 10^{-13}$
344	$(2.6 \pm 0.9) \times 10^{-13}$

[a]errors are 2σ.

The observed rate coefficient is larger than the second-order rate coefficient of just the CH_3O_2 recombination reaction (R4), k_4, as the methoxy radicals generated by channel R4.b react rapidly with molecular oxygen, which is present in large excess, 5×10^{18} molecules cm^{-3}, to produce HO_2 (reaction R2), which in turn reacts with another CH_3O_2 radical (reaction R5). As each HO_2 radical consumes one CH_3O_2 species (reaction R5) on the time scale of reaction R4, k_4 is derived from k_{obs} as follows:[7,11]

$$k_{obs} = k_4(1 + r_{CH3O}) \quad (1)$$

where r_{CH3O} is the branching ratio for the reaction channel R4.b. The applicability of eq 1 in the analysis of the kinetic data generated by the HIRAC experiments was demonstrated by modeling the observed temporal decays using a variety of CH_3O_2 and HO_2 concentrations representative for the HIRAC experiments and incorporating a heterogeneous loss of HO_2 in the model relevant for the experiments:[22,23] $k_{loss} = 0.01-0.1$ s^{-1}. The results showed that the removal of HO_2 by wall loss is negligible and thus can be excluded from the model.[22]

Figure 3 shows the determined temperature dependence for k_4. At all temperatures employed, the values of k_4 obtained using both k_{obs} and r_{CH3O} determined in this work are practically the same as the k_4 values obtained using k_{obs} determined in this work and r_{CH3O} given by the evaluation of Tyndall et al.,[21] which is recommended by JPL.[6] Using the value of $r_{CH3O} = 0.34 \pm 0.05$ determined at 295 K in this work the rate coefficient of the overall reaction $k_4(295\ K) = (2.0 \pm 0.7) \times 10^{-13}$ cm^3 molecule^{-1} s^{-1} (uncertainties at 2σ level). Using the value of $r_{CH3O}(295\ K) = 0.36 \pm 0.12$ recommended by Tyndall et al.[21] does not change the result at this level of precision: $k_4(295\ K) = (2.0 \pm 0.9) \times 10^{-13}$ cm^3 molecule^{-1} s^{-1} (uncertainties quoted at 2σ level). The negative temperature

https://doi.org/10.1021/acs.jpca.2c04968
J. Phys. Chem. A 2022, 126, 7639−7649

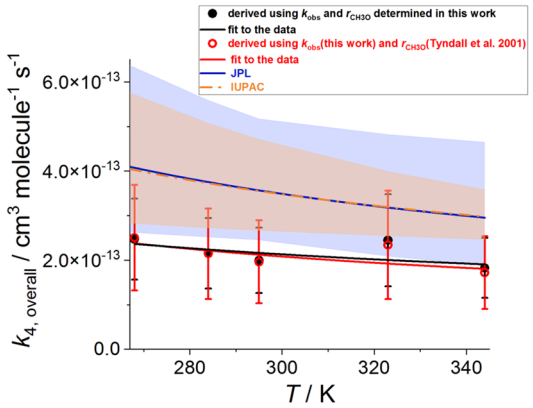

Figure 3. Temperature dependence of the overall rate coefficient of the CH_3O_2 self-reaction (R4), k_4. The data generated using k_{obs} and r_{CH3O} obtained in this work (black circles) are plotted with the data generated using k_{obs} measured by this work and r_{CH3O} given by the evaluation of Tyndall et al.[21] (open red circles) and k_4 recommended by JPL (blue line and shading)[6] and IUPAC (orange dashed line and shading).[5] The blue and orange shadings show the 2σ uncertainties in the JPL and IUPAC recommendations. The results of the fit to the data are $k_4 = (9.1 \pm 5.3) \times 10^{-14} \times \exp((252 \pm 174)/T)$ cm^3 molecule^{-1} s^{-1} (black line) and $k_4 = (6.8 \pm 4.1) \times 10^{-14} \times \exp((335 \pm 179)/T)$ cm^3 molecule^{-1} s^{-1} (red line). The parametrization of the temperature dependence of k_4 recommended by JPL and IUPAC are k_4(JPL) = $9.5 \times 10^{-14} \times \exp(390/T)$ cm^3 molecule^{-1} s^{-1}[6] and k_4(IUPAC) = $1.03 \times 10^{-13} \times \exp((365)/T)$ cm^3 molecule^{-1} s^{-1}.[5]

dependence obtained employing r_{CH3O} determined in this work can be characterized by $k_4 = (9.1 \pm 5.3) \times 10^{-14} \times \exp((252 \pm 174)/T)$ cm^3 molecule^{-1} s^{-1}. Figure 3 compares the result of this work with k_4 vs T recommended by JPL and IUPAC. The JPL and IUPAC recommendations are similar to each other: k_4(JPL) = $9.5 \times 10^{-14} \times \exp(390/T)$ cm^3 molecule^{-1} s^{-1}[6] and k_4(IUPAC) = $1.03 \times 10^{-13} \times \exp((365 \pm 200)/T)$ cm^3 molecule^{-1} s^{-1}.[5] On average, the results of this work are ∼40% lower than the values calculated using the JPL and IUPAC recommendations. However, the results of this work have overlapping error limits at the 2σ level with both recommendations.

The previous studies upon which the JPL[6] and IUPAC[5] recommendations are based utilized the UV-absorption of CH_3O_2 at fixed wavelengths in the range ∼210−270 nm (typically 250 nm) usually to determine the ratio between the observed rate coefficient and the absorption cross-section of CH_3O_2, k_{obs}/σ_{CH3O2}.[5,6] The values used for σ_{CH3O2} by the previous UV-absorption studies vary significantly, between $(2.5-4.8) \times 10^{-18}$ cm^2 molecule^{-1} at 250 nm, leading to a large variation in k_{obs} across the studies, which at 298 K ranges between $k_{obs} = (3.0-5.9) \times 10^{-13}$ cm^3 molecule^{-1} s^{-1}.[7−14] The 2020 JPL[6] evaluation report recommends the cross sections obtained by the re-evaluation of Tyndall et al. in 2001[21] of the previous reported UV-absorption spectra. At 250 nm Tyndall et al.[21] recommend $\sigma_{CH3O2(250\ nm)} = 3.8 \times 10^{-18}$ cm^2 molecule^{-1}. Our calculations show that using σ_{CH3O2} reported by Tyndall et al.[21] and the ratios k_{obs}/σ_{CH3O2} found in the previous kinetic studies,[7−11,13,14] the range of the values of k_{obs} at 298 K is reduced to $(4.1-5.1) \times 10^{-13}$ cm^3 molecule^{-1} s^{-1}. The present result at 298 K, $k_{obs} = 2.9 \times 10^{-13}$ cm^3 molecule^{-1} s^{-1}, is 30% smaller than the lowest value of 4.1×10^{-13} cm^3 molecule^{-1} s^{-1} and 40% lower than the JPL[6] and IUPAC[5] recommendations of $k_{obs} = 4.8 \times 10^{-13}$ cm^3 molecule^{-1} s^{-1}.

There is a significant difference between the results obtained here and the recommendations,[5,6] and here we explore possible reasons for this discrepancy. The previous studies used either the flash photolysis (FP) technique[7−11] or the molecular modulation (MM) method[12−14] to generate CH_3O_2 radicals employing photolytic mixtures of $CH_4/Cl_2/O_2$. The discrepancy between k_{obs} determined in here and the results reported in the FP studies[7−11] could be due to unaccounted secondary chemistry of CH_3O_2 due to the high radical concentrations, on the order of $[CH_3O_2]$ of $10^{13}-10^{14}$ molecules cm^{-3}, and/or unaccounted spectral interferences. The MM experiments[12−14] used 1−2 orders of magnitude lower concentrations of CH_3O_2 than $[CH_3O_2]$ in the FP studies,[7−11] i.e., concentrations on the order 10^{12} molecules cm^{-3}, to minimize the impact of the secondary chemistry on k_{obs}. However, as this method consisted of modulating the photolysis and hence the production of radicals by alternating the time with the lamps switched on and the time with the lamps turned off, a potential important source of error was the buildup of products absorbing in the UV range of the measurements (see below). The contributions of the absorbing products (see below) were subtracted from the overall absorbance measured by the MM experiments[12,14] to extract the absorbance of CH_3O_2, and thus the extracted absorbance depended on the concentrations and the cross sections attributed to the products. Note that the LIF method is selective and more sensitive, with a limit of detection for CH_3O_2 of 2.0×10^9 molecules cm^{-3} for a signal-to-noise ratio of 2, 1 s averaging time of the online data points measured during the kinetic decay, and 60 s averaging period for the offline data points recorded at the end of the experiment. Therefore, the LIF method requires significantly lower radical concentrations than the FP and MM studies; here, $[CH_3O_2]_0 = (0.1-1) \times 10^{12}$ molecules cm^{-3}, which helps to minimize potential secondary chemistry.

The FP studies[7−11] typically derived the k_{obs}/σ_{CH3O2} ratio fitting either eq 10 or eq 11 to the measured optical absorbance (A_t) or absorption coefficient (α_t) at/around 250 nm.

$$\frac{1}{A_t} = \frac{1}{A_0} + 2\frac{k_{obs}}{\sigma_{CH3O2} l} t \quad (10)$$

$$\frac{1}{\alpha_t} = \frac{1}{\alpha_0} + 2\frac{k_{obs}}{\sigma_{CH3O2}} t \quad (11)$$

Here A_0 and α_0 are the absorbance and the absorption coefficient at the time zero of the reaction, respectively, and l is the total optical path length.

To investigate the potential impact of the secondary chemistry on the CH_3O_2 kinetic decays in the FP studies[7−11] numerical simulations were performed using a reaction system at 298 K described in the Supporting Information (Table S1). The previous kinetic studies of the CH_3O_2 recombination reaction[7−14] did not investigate the impact of the CH_3O_2 reaction with the ClO radicals produced by the CH_3O_2 + Cl reaction on the CH_3O_2 kinetic decay. The kinetics of the CH_3O_2 + Cl reaction[34,35] was studied in the years around 1995 and thus after all the previous kinetic studies of the CH_3O_2 self-reaction (1980−1990).[5,6] The CH_3O_2 + Cl reaction is fast producing ClO (rate coefficient of 7.7×10^{-11} cm^3 molecule^{-1} s^{-1} at 298 K).[34] The generated ClO radicals predominantly react with CH_3O_2 with an overall rate coefficient of 2.4×10^{-12} cm^3 molecule^{-1} s^{-1} at 298 K.[6]

https://doi.org/10.1021/acs.jpca.2c04968
J. Phys. Chem. A 2022, 126, 7639−7649

The simulations used $k_4 = 2.1 \times 10^{-13}$ cm^3 molecule^{-1} s^{-1} as determined in this work and $r_{CH3O} = 0.37$.[5,6] The Supporting Information shows examples of the results of the numerical simulations using concentrations representative for the FP studies:[7−11] $[CH_4]_0 = 5 \times 10^{17}$ molecules cm^{-3} and $[Cl]_0 = 1.4 \times 10^{14}$ molecules cm^{-3}. As the Cl + CH_4 reaction is relatively slow (rate coefficient = 1.0×10^{-13} cm^3 molecule^{-1} s^{-1} at 298 K)[36] about 7% of the Cl atoms react with CH_3O_2 to produce ClO. Subsequently ClO predominantly reacts with CH_3O_2 (peak $[CH_3O_2] = 1.0 \times 10^{14}$ molecules cm^{-3} as shown in the Supporting Information). Therefore, fitting eq 8 to the CH_3O_2 temporal decay simulated using the mechanism which includes the secondary chemistry results in k_{obs}(fit) = (3.8 ± 0.1) × 10^{-13} cm^3 molecule^{-1} s^{-1}. Using eq 9, k_4(fit) = 2.8×10^{-13} cm^3 molecule^{-1} s^{-1} is obtained, which is 33% higher than the value of k_4 determined from this work and used as an input in the numerical simulations, k_4(simulations) = 2.1×10^{-13} cm^3 molecule^{-1} s^{-1}. To investigate the sensitivity of the results to the presence of the CH_3O_2 + ClO reaction in the chemical mechanism used, the simulations with $[CH_4]_0 = 5 \times 10^{17}$ molecules cm^{-3} and $[Cl]_0 = 1.4 \times 10^{14}$ molecules cm^{-3} were repeated, but this time in the absence of the CH_3O_2 + ClO reaction. Without the CH_3O_2 + ClO reaction, k_{obs}(fit) = (3.0 ± 0.1) × 10^{-13} cm^3 molecule^{-1} s^{-1} resulting in k_4(fit) = 2.2×10^{-13} cm^3 molecule^{-1} s^{-1} being obtained, which is almost the same with the value used as input in the simulations, k_4(simulations) = 2.1×10^{-13} cm^3 molecule^{-1} s^{-1}. Hence, for $[CH_4]_0 = 5 \times 10^{17}$ molecules cm^{-3} and $[Cl]_0 = 1.4 \times 10^{14}$ molecules cm^{-3}, the values of k_{obs} and k_4 obtained from the fit to the simulated CH_3O_2 decay are considerably larger if the secondary chemistry is included to generate the decay. As the studies using the flash photolysis technique[7−11] typically employed ∼$[CH_4]_0 = 10^{17}$ molecules cm^{-3} and ∼$[Cl]_0 = 10^{14}$ molecules cm^{-3} the studies significantly overestimated k_{obs} and thus k_4.

In the present study the concentrations of $[CH_3O_2]$, [Cl], and [ClO] were in a steady-state with the lamps turned on, and the CH_3O_2 decays were generated by switching the lamps off. Numerical simulations were performed over 5 min to mimic the chemistry with the lamps turned on using $[CH_4]_0 = 3.0 \times 10^{17}$ molecules cm^{-3} with $[Cl_2]_0 = 3.0 \times 10^{14}$ molecules cm^{-3} representative for the present study and adding the Cl_2 photolysis to the chemistry mechanism including the CH_3O_2 + Cl and CH_3O_2 + ClO reactions (Supporting Information). After 5 min with the lamps on, $[CH_3O_2] = 5 \times 10^{11}$ molecules cm^{-3}, $[Cl] = 7.0 \times 10^6$ molecules cm^{-3}, and $[ClO] = 2.4 \times 10^8$ molecules cm^{-3}. The concentrations of all the species in the chemistry mechanism obtained after 5 min were input into numerical simulations using the same chemistry mechanism except without Cl_2 photolysis to mimic the chemistry during the time with the lamps turned off. Virtually all Cl atoms and ClO radicals were removed on a time scale of hundreds of microseconds and seconds, respectively. As $[Cl]_0 = 7.0 \times 10^6$ molecules cm^{-3} and $[ClO]_0 = 2.4 \times 10^8$ molecules cm^{-3}, and hence orders of magnitude lower than $[Cl]_0 = 1.4 \times 10^{14}$ molecules cm^{-3} and a peak of $[ClO] = 1.0 \times 10^{13}$ molecules cm^{-3} in the simulations using concentrations representative for the FP studies,[7−11] the simulated CH_3O_2 decays were not impacted by the chlorine species secondary chemistry (Figure S3). The fit of eq 9 to the CH_3O_2 decay provided a value of k_{obs}(fit) = (3.0 ± 0.1) × 10^{-13} cm^3 molecule^{-1} s^{-1} at 298 K, which results in k_4(fit) = 2.2×10^{-13} cm^3 molecule^{-1} s^{-1}, i.e., practically the same as the value measured by the present experiments $k_4 = 2.1 \times 10^{-13}$ cm^3 molecule^{-1} s^{-1}. Therefore, no impact by the secondary chemistry of CH_3O_2 included in the simulations (Supporting Information) on the value determined for k_4 was found in the present study. Hence in the absence of secondary chemistry the value of k_4, as determined in this work, is considerably lower than k_4 when the secondary chemistry is present as a result of much higher initial [Cl] concentrations.

We now consider potential spectral interferences in previous work which monitored CH_3O_2 concentrations using UV absorption. At the typical λ = 250 nm used to monitor the CH_3O_2 absorption by the FP studies,[7−11] the cross-section of ClO, $\sigma_{ClO} = 3.5 \times 10^{-18}$ cm^2 molecule^{-1}[6] and the cross-section of CH_3O_2, $\sigma_{CH3O2} = 3.8 \times 10^{-18}$ cm^2 molecule^{-1}[21] are similar, and hence numerical simulations were used to investigate the impact of any ClO spectral interference on the results of the FP studies. The concentrations of the species generated by numerical simulations using the representative concentrations for the FP studies of $[CH_4]_0 = 5 \times 10^{17}$ molecules cm^{-3} and $[Cl]_0 = 1.4 \times 10^{14}$ molecules cm^{-3} in the model that includes the CH_3O_2 + ClO reaction were multiplied with their respective cross sections[6,21] to obtain the absorption coefficients of CH_3O_2 and ClO:

$$\alpha_{i,t} = \sigma_i [i]_t \quad (12)$$

where $\alpha_{i,t}$ is the absorption coefficient of species i (CH_3O_2 or ClO) at reaction time t, σ_i is the absorption cross-section of species i at 250 nm and $[i]_t$ is the concentration of species i at time t. Figure S4 in the Supporting Information shows the generated $\alpha_{CH3O2,t}$ and $\alpha_{ClO,t}$ and their sum, $\Sigma\alpha_{i,t} = \alpha_{CH3O2,t} + \alpha_{ClO,t}$. The results (Figure S4) show that there is a minor contribution of $\alpha_{ClO,t}$ to $\Sigma\alpha_{i,t}$ at the start of the reaction, i.e., ∼8% in the first millisecond of the reaction, which drops to 3% at t = 10 ms. The fit of the eq 11 (see above) to $\Sigma\alpha_{i,t}$ vs time resulted in k_{obs}/σ_{CH3O2}. Using $\sigma_{CH3O2} = 3.8 \times 10^{-18}$ cm^2 molecule^{-1}[21] a value of k_{obs} = (3.9 ± 0.1) × 10^{-13} cm^3 molecule^{-1} s^{-1} is obtained, which is 3% higher than k_{obs} given fitting eq 9 to the temporal decay of $[CH_3O_2]$ generated by the same numerical simulations (Figure S1). The result suggests that there was no significant optical interference due to the ClO absorption which impacted the previous determinations of k_{obs} using the FP technique.[7−11]

The molecular modulation (MM) studies[12−14] used the time-resolved modulated UV-absorption (absorption waveform) generated in the range 210−270 nm via switching the photolysis lamps on and off with a typical frequency of 10^{-1} Hz (order of magnitude) to determine k_{obs} and σ_{CH3O2}. The absorption waveform consisted of an initial rise followed by a pseudo-steady-state and then a decay during the dark phase of the modulation period.[12−14] The modulated absorption components depended on a relatively large number of parameters: illumination time, rate of Cl_2 photolysis, kinetic parameters, and absorbing species cross sections.[12−14] Photolytic mixtures of $CH_4/Cl_2/O_2$ were flowed through the reactor to minimize the buildup of the products. However, the residence times of the gases in the reaction cell were relatively long, for example, 35 and 60 s.[13,14] The contributions of the absorbing products accumulating over the photolysis cycles was calculated and subtracted from the observed absorption to derive the modulated absorption of CH_3O_2.[12,14] The contribution of the products were important in the range 210−250 nm where the cross sections of HO_2 (formed by reaction R2 and the reactions of Cl with the products CH_3OH

https://doi.org/10.1021/acs.jpca.2c04968
J. Phys. Chem. A 2022, 126, 7639−7649

and CH_2O) and CH_3OOH (produced by the CH_3O_2 + HO_2 reaction) increases rapidly with decreasing λ.[6] However, the cross sections of HO_2 and/or CH_3OOH were significantly overestimated in the MM studies.[12−14] The references cited for the cross-section of HO_2 by Cox and Tyndall[12] reported σ_{HO2} larger than the JPL recommendations[6] by 60−70% in the range 210−250 nm[37] and by ∼10% between 210−220 nm.[38] The cross-section of HO_2[39] used by Simon et al.[14] is ∼30% larger than the JPL recommendation[6] between 210−240 nm and by ∼60% at 250 nm. Both the studies of Cox and Tyndall[12] and Jenkin et al.[13] employed values for σ_{CH3OOH} at least 40−50% higher than the JPL recommendation in the range 210−250 nm.[6] An overestimation of the contributions of these species to the measured absorbance results in an underestimation of the CH_3O_2 absorbance, A_{CH3O2}, which in turn results in an overestimation of k_{obs}/σ_{CH3O2} (eq 10).

In addition, the CH_3O_2 loss to the walls of the reaction cell were not accounted for by neither the FP studies[7−11] nor the MM studies[12−14] and could also result in an overestimation of k_{obs}. As the CH_3O_2 self-reaction is slow, the wall-loss could significantly contribute to the overall CH_3O_2 removal in the previous studies.

DISCUSSION OF THE FAGE INSTRUMENT CALIBRATION

As LIF is not an absolute detection method, the FAGE instrument required calibration and a calibration factor, $C_{CH_3O_2}$, is used to convert the measured signal, $S_{CH_3O_2}$, to the CH_3O_2 concentration:

$$[CH_3O_2] = \frac{S_{CH_3O_2}}{C_{CH_3O_2}} \quad (5)$$

To calibrate FAGE, CH_3O_2 radicals were generated in known concentrations employing the 184.9 nm photolysis of water vapor in synthetic air followed by the complete conversion of the generated OH radicals to CH_3O_2 by reaction with CH_4 in a large excess in the presence of O_2. Previous work described in detail the water vapor method of calibration and the uncertainties in the calibration factor, $C_{CH_3O_2}$(water vapor method).[22] As seen previously,[22] in this work an overall 34% error at 2σ level was obtained for $C_{CH_3O_2}$(water vapor method) combining the systematic and statistical uncertainties. Similar overall errors, 31% and 36%, were reported for C_{HO_2}(water vapor method) previously.[28,30]

The photolysis of water vapor at 184.9 nm represents the most common method used to generate accurate concentrations of OH and HO_2. The method has been applied for many years for the calibration of FAGE instruments.[24−26] The reliability of the method has been confirmed by intercomparisons with alternative methods of calibration for OH and HO_2. The calibration of OH using the water vapor photolysis and the OH calibration based on the generation of OH by ozone reactions with alkenes have been found to agree within their experimental uncertainties.[40] Very good agreement (difference within 1−13%) has been obtained by comparing the OH measurements in the SAPHIR atmospheric simulation chamber using a number of FAGE instruments and instruments employing differential optical laser absorption spectroscopy (DOAS) and chemical ionization mass spectrometry (CIMS).[41,42] In the case of HO_2, C_{HO_2}(water vapor method) and the calibration factor obtained analyzing the kinetic decay of HO_2 by its self-reaction generated in HIRAC, C_{HO_2}(kinetic method), were found in a very good agreement (difference within 8%).[28,30] However, a discrepancy within ∼40% was found between $C_{CH_3O_2}$(water vapor method) and the CH_3O_2 calibration factor determined using the kinetics of the second-order recombination of CH_3O_2 observed in HIRAC and $k_{obs}(298\ K) = 4.8 \times 10^{-13}$ cm^3 molecule^{-1} s^{-1},[5,6] $C_{CH_3O_2}$(kinetic method).[22,23] As the error in the fraction of OH which is converted to CH_3O_2 upon the addition of methane in the water vapor method is minor (4% at 2σ level),[22] the discrepancy between the two calibration methods can be attributed to an overestimation of the reported value of k_{obs} for the CH_3O_2 self-reaction at 298 K.[5,6] The ∼40% difference in $C_{CH_3O_2}$(kinetic method) and $C_{CH_3O_2}$(water vapor method) resulted in different values for the gradient of the correlation plot of $[CH_3O_2]$ measured by FAGE (y-axis) as a function of $[CH_3O_2]$ measured by near-infrared cavity ring down spectroscopy, CRDS (x-axis), at 1000 mbar of synthetic air using the sensitivities from the two methods of calibration of FAGE: 1.35 ± 0.07 (water vapor calibration) and 0.92 ± 0.05 (kinetic method of calibration).[23] The results show a significantly better agreement with the kinetic method than with the water vapor method. A very good level of agreement between the FAGE and CRDS measurements of CH_3O_2 was also obtained using the kinetic method for FAGE calibration at 100 mbar of synthetic air and 80 mbar of 3:1 He:O_2 mixture. The very good agreement achieved under all conditions when the kinetic method was employed for the FAGE calibration was expected as the kinetic method was also used to determine the absorption cross section of CH_3O_2 from the temporal decays of the optical absorption coefficient of CH_3O_2 and hence calibrate the CRDS method. Therefore, with both FAGE and CRDS calibrated using the same method, the intercomparison was not subject to any error in the rate coefficient, k_{obs} for the CH_3O_2 self-reaction, and the obtained very good agreement provides a validation of the FAGE (water vapor) method to determine concentrations of CH_3O_2. The present result at 298 K, $k_{obs} = 2.9 \times 10^{-13}$ cm^3 molecule^{-1} s^{-1}, shows a 40% reduction in the reported value of $k_{obs} = 4.8 \times 10^{-13}$ cm^3 molecule^{-1} s^{-1}.[5,6] A reduction of 40% in the reported k_{obs} would bring $[CH_3O_2]_{CRDS}$ generated using the kinetic method of calibration into agreement with $[CH_3O_2]_{FAGE}$ determined using the water vapor method.[23] Therefore, the FAGE−CRDS intercomparison also suggests that $k_{obs} = 2.9 \times 10^{-13}$ cm^3 molecule^{-1} s^{-1} and thus $k_4 = 2.1 \times 10^{-13}$ cm^3 molecule^{-1} s^{-1} at 298 K, consistent with the values found in the present study.

CONCLUSIONS

Experiments were carried out in the range 268−344 K and at 1000 mbar to measure CH_3OH and CH_2O generated by the CH_3O_2 self-reaction in HIRAC using *in situ* FTIR detection to determine the product branching ratios in the self-reaction. The chemistry was initiated using photolysis of $Cl_2/CH_4/N_2/O_2$ mixtures (photolysis range: λ = 350−400 nm). The temperature dependence of the product branching ratio of the reaction channel producing CH_3O can be described as $r_{CH3O} = 1/\{1 + [\exp(600 \pm 170)/T]/(3.9 \pm 2.2)\}$. At 295 K $r_{CH3O(this\ work)} = 0.34 \pm 0.05$, in agreement with the recommendations of JPL[6] and IUPAC:[5] $r_{CH3O(JPL)} = 0.36 \pm$

https://doi.org/10.1021/acs.jpca.2c04968
J. Phys. Chem. A 2022, 126, 7639−7649

0.12 and $r_{CH3O(IUPAC)}$ = 0.36 ± 0.17. This is the second experimental study of the temperature dependence of the product branching ratios in a range including temperatures relevant for atmospheric chemistry. The positive temperature dependence found for r_{CH3O} is less marked than the increase in r_{CH3O} with temperature measured by the previous study performed in a temperature range around 298 K (223−333 K), which used matrix isolation FTIR.[20] The results of the present work for product branching agree well with the values obtained by Horie et al.[20] at 295, 323, and 344 K. By decreasing the temperature, the present results are increasingly higher than the results reported by Horie et al.[20] with a positive deviation of 22% at 268 K.

The kinetics of the CH_3O_2 self-reaction has been studied coupling a FAGE instrument to HIRAC to carry out time-resolved measurements of the CH_3O_2 concentrations during the reaction. Second-order decays of CH_3O_2 were generated by turning the chamber lamps off. The observed rate coefficient at 295 K and 1000 mbar was k_{obs} = (2.7 ± 0.9) × 10^{-13} cm^3 $molecule^{-1}$ s^{-1}. Using $k_{obs}(295\ K) = k_4(1 + r_{CH3O})$ with $r_{CH3O(this\ work,\ 295\ K)}$ = 0.34 ± 0.05 the second-order rate coefficient for the self-reaction at 295 K and 1000 mbar is k_4 = (2.0 ± 0.7) × 10^{-13} cm^3 $molecule^{-1}$ s^{-1}; employing the recommended value of 0.36 for r_{CH3O} at 295 K by JPL[6] and IUPAC[5] does not change the result. The result at 295 K is is ∼40% lower than the IUPAC and JPL recommendations: k_4 = 3.5 × 10^{-13} cm^3 $molecule^{-1}$ s^{-1}. The temperature dependence of the overall rate coefficient can be parametrized as k_4 = (9.1 ± 5.3) × 10^{-14} × exp((252 ± 174)/T) cm^3 $molecule^{-1}$ s^{-1}. The present results have overlapping error limits at the 2σ level with both JPL and IUPAC recommendations. However, on average the results of this work are ∼40% lower than the values calculated using the JPL[6] recommendation for the temperature dependence (k_4 = 9.5 × 10^{-14} × exp(390/T) cm^3 $molecule^{-1}$ s^{-1}) and the values obtained employing the temperature dependence recommended by IUPAC,[5] k_4 = 1.03 × 10^{-13} × exp((365 ± 200)/T) cm^3 $molecule^{-1}$ s^{-1}.

The previous kinetic studies utilized UV−absorption spectroscopy and may be impacted by secondary chemistry owing to the high radical concentrations generated in the reaction mixtures. Chemical modeling using the conditions of the previous studies and which included secondary chemistry of Cl species showed that the secondary chemistry increases the value of k_4 obtained significantly. The FAGE method detects CH_3O_2 sensitively, with a limit of detection of 2.0 × 10^9 molecules cm^{-3} for a signal-to-noise ratio of 2, 1 s online averaging time, and 60 s offline averaging period. Therefore, the experiments reported here required a few orders of magnitude lower concentrations of CH_3O_2 than [CH_3O_2] used in the UV−absorption studies and the impact of the secondary chemistry on the kinetic decays obtained by this work is negligible. In addition, the FAGE method probes CH_3O_2 selectively, in the absence of any interference from other species.

Numerical models predict that CH_3O_2 is the most abundant RO_2 species in the atmosphere. Even though CH_3O_2 has not been selectively measured in the atmosphere so far, its concentration at daytime has been estimated to peak in the range of daytime peak [HO_2], i.e., at 10^7−10^8 molecules cm^{-3}.[43−45] The atmospheric fate of CH_3O_2 is typically dominated by the reaction with NO, with the CH_3O_2 + HO_2 reaction becoming the main daytime loss of CH_3O_2 under low NO_x levels. As CH_3O_2 and HO_2 reach similar levels at daytime and 298K, $k_{CH3O2+HO2}$ (5.2 × 10^{-12} cm^3 $molecule^{-1}$ s^{-1}) is ∼15 times faster than the JPL and IUPAC recommendations for k_4 (3.5 × 10^{-13} cm^3 $molecule^{-1}$ s^{-1})[5,6] and ∼25 times higher than $k_{4(CH3O2+CH3O2)}$ determined in this work (2.1 × 10^{-13} cm^3 $molecule^{-1}$ s^{-1}) the inclusion of the present $k_{obs(CH3O2+CH3O2)}$ value in the atmospheric models might not impact significantly the daytime radical budget predicted by the models. However, at night-time it has been predicted that the self-reaction is the dominant removal of CH_3O_2 due to a rapid loss of HO_2 under dark conditions[46] and thus the atmospheric impacts of the present result need to be investigated.

■ ASSOCIATED CONTENT

Supporting Information

The Supporting Information is available free of charge at https://pubs.acs.org/doi/10.1021/acs.jpca.2c04968.

Results of numerical simulations using a complex chemistry system and details of determination of the branching ratios in the CH_3O_2 self-reaction as a function of temperature (PDF)

■ AUTHOR INFORMATION

Corresponding Author

Dwayne E. Heard − *School of Chemistry, University of Leeds, Leeds LS2 9JT, United Kingdom;* orcid.org/0000-0002-0357-6238; Phone: +44 113 343 6471; Email: d.e.heard@leeds.ac.uk

Authors

Lavinia Onel − *School of Chemistry, University of Leeds, Leeds LS2 9JT, United Kingdom*

Alexander Brennan − *School of Chemistry, University of Leeds, Leeds LS2 9JT, United Kingdom*

Freja F. Østerstrøm − *School of Chemistry, University of Leeds, Leeds LS2 9JT, United Kingdom;* Present Address: School of Engineering and Applied Sciences, Harvard University, Cambridge, MA 02138, USA and Department of Chemistry, University of Copenhagen, 2100 Copenhagen Ø, Denmark; orcid.org/0000-0003-4125-3365

Ellie Cooke − *School of Chemistry, University of Leeds, Leeds LS2 9JT, United Kingdom*

Lisa Whalley − *School of Chemistry, University of Leeds, Leeds LS2 9JT, United Kingdom; National Centre for Atmospheric Science, University of Leeds, LS2 9JT, United Kingdom*

Paul W. Seakins − *School of Chemistry, University of Leeds, Leeds LS2 9JT, United Kingdom;* orcid.org/0000-0002-4335-8593

Complete contact information is available at: https://pubs.acs.org/10.1021/acs.jpca.2c04968

Notes

The authors declare no competing financial interest.

■ ACKNOWLEDGMENTS

The authors would like to thank the Natural Environment Research Council (NERC) for funding (grant reference NE/M011208/1) and the National Centre for Atmospheric Science. AB thanks to NERC for a studentship awarded in the framework of the SPHERES doctoral training programme (NE/L002574/1). F.F.Ø. thanks the Carlsberg Foundation for

support through the Carlsberg Foundation Internationalisation Fellowship, grant numbers CF16-0493 and CF17-0608.

REFERENCES

(1) Orlando, J. J.; Tyndall, G. S. Laboratory studies of organic peroxy radical chemistry: an overview with emphasis on recent issues of atmospheric significance. *Chem. Soc. Rev.* **2012**, *41* (19), 6294−6317.
(2) Kohse-Hoinghaus, K. Combustion in the future: The importance of chemistry. *Proc. Combust. Inst.* **2021**, *38* (1), 1−56.
(3) Zador, J.; Taatjes, C. A.; Fernandes, R. X. Kinetics of elementary reactions in low-temperature autoignition chemistry. *Prog. Energy Combust.* **2011**, *37* (4), 371−421.
(4) Tyndall, G. S.; Wallington, T. J.; Ball, J. C. FTIR product study of the reactions CH_3O_2+CH_3O_2 and CH_3O_2+O_3. *J. Phys. Chem. A* **1998**, *102* (15), 2547−2554.
(5) Atkinson, R.; Baulch, D. L.; Cox, R. A.; Crowley, J. N.; Hampson, R. F.; Hynes, R. G.; Jenkin, M. E.; Rossi, M. J.; Troe, J. Evaluated kinetic and photochemical data for atmospheric chemistry: Volume II - gas phase reactions of organic species. *Atmos. Chem. Phys.* **2006**, *6*, 3625−4055.
(6) Burkholder, J. B.; Sander, S. P.; Abbatt, J. P. D.; Barker, J. R.; Cappa, C.; Crounse, J. D.; Dibble, T. S.; Huie, R. E.; Kolb, C. E.; Kurylo, et al.. Chemical kinetics and photochemical data for use in atmospheric studies - Evaluation number 19. available at http://jpldataeval.jpl.nasa.gov/, Access 10 May 2022.
(7) Lightfoot, P. D.; Lesclaux, R.; Veyret, B. Flash photolysis study of the CH_3O_2 + CH_3O_2 reaction: Rate constants and branching ratios from 248 to 573 K. *J. Phys. Chem.* **1990**, *94* (2), 700−707.
(8) Sander, S. P.; Watson, R. T. Kinetic studies of the reactions of CH_3O_2 with NO, NO_2 and CH_3O_2 at 298 K. *J. Phys. Chem.* **1980**, *84* (13), 1664−1674.
(9) McAdam, K.; Veyret, B.; Lesclaux, R. UV absorption spectra of HO_2 and CH_3O_2 radicals and the kinetics of their mutual reactions ant 298 K. *Chem. Phys. Lett.* **1987**, *133* (1), 39−44.
(10) Kurylo, M. J.; Wallington, T. J. The temperature dependence of the rate constant for the gas phase disproportionation reaction of CH_3O_2 radicals. *Chem. Phys. Lett.* **1987**, *138* (6), 543−547.
(11) Sander, S. P.; Watson, R. T. Temperature dependence of the self-reaction of CH_3O_2 radicals. *J. Phys. Chem.* **1981**, *85* (20), 2960−2964.
(12) Cox, R. A.; Tyndall, G. S. Rate constants for the reactions of CH_3O_2 with HO_2, NO and NO_2 using molecular modulation spectrometry. *J. Chem. Soc. Faraday Trans II* **1980**, *76*, 153−163.
(13) Jenkin, M. E.; Cox, R. A.; Hayman, G. D.; Whyte, L. J. Kinetic study of the reactions CH_3O_2 + CH_3O_2 and CH_3O_2 + HO_2 using molecular modulation spectroscopy. *J. Chem. Soc. Faraday Trans. II* **1988**, *84*, 913−930.
(14) Simon, F. G.; Schneider, W.; Moortgat, G. K. UV absorption spectrum of the methylperoxy radical and the kinetics of its disproportionation reaction at 300 K. *Int. J. Chem. Kinet.* **1990**, *22* (8), 791−812.
(15) Tyndall, G. S.; Wallington, T. J.; Ball, J. C. FTIR product study of the reactions CH_3O_2 + CH_3O_2 and CH_3O_2 + O_3. *J. Phys. Chem. A* **1998**, *102* (15), 2547−2554.
(16) Weaver, J.; Meagher, J.; Shortridge, R.; Heicklen, J. Oxidation of acetyl radicals. *J. Photochem.* **1975**, *4* (5−6), 341−360.
(17) Selby, K.; Waddington, D. J. Reactions of oxygenated radicals in the gas-phase 0.4. reactions of methylperoxyl and methoxyl radicals. *J. Chem. Soc.-Perkin Trans. 2* **1979**, *9*, 1259−1263.
(18) Kan, C. S.; Calvert, J. G.; Shaw, J. H. Reactive channels of the CH_3O_2-CH_3O_2 reaction. *J. Phys. Chem.* **1980**, *84* (25), 3411−3417.
(19) Niki, H.; Maker, P. D.; Savage, C. M.; Breitenbach, L. P. Fourier transform infrared studies of the self-reaction of CH_3O_2 radicals. *J. Phys. Chem.* **1981**, *85* (7), 877−881.
(20) Horie, O.; Crowley, J. N.; Moortgat, G. K. Methylperoxy relf-reaction: Products and branching ratio between 223 and 333 K. *J. Phys. Chem.* **1990**, *94* (21), 8198−8203.
(21) Tyndall, G. S.; Cox, R. A.; Granier, C.; Lesclaux, R.; Moortgat, G. K.; Pilling, M. J.; Ravishankara, A. R.; Wallington, T. J. Atmospheric chemistry of small organic peroxy radicals. *J. Geophys. Res. -Atmos.* **2001**, *106* (D11), 12157−12182.
(22) Onel, L.; Brennan, A.; Seakins, P. W.; Whalley, L.; Heard, D. E. A new method for atmospheric detection of the CH_3O_2 radical. *Atmos. Meas. Technol.* **2017**, *10* (10), 3985−4000.
(23) Onel, L.; Brennan, A.; Gianella, M.; Hooper, J.; Ng, N.; Hancock, G.; Whalley, L.; Seakins, P. W.; Ritchie, G. A. D.; Heard, D. E. An intercomparison of CH_3O_2 measurements by fluorescence assay by gas expansion and cavity ring-down spectroscopy within HIRAC (Highly Instrumented Reactor for Atmospheric Chemistry). *Atmos. Meas. Technol.* **2020**, *13* (5), 2441−2456.
(24) Heard, D. E.; Pilling, M. J. Measurement of OH and HO_2 in the troposphere. *Chem. Rev.* **2003**, *103* (12), 5163−5198.
(25) Stone, D.; Whalley, L. K.; Heard, D. E. Tropospheric OH and HO_2 radicals: field measurements and model comparisons. *Chem. Soc. Rev.* **2012**, *41* (19), 6348−6404.
(26) Wang, G. Y.; Iradukunda, Y.; Shi, G. F.; Sanga, P.; Niu, X. L.; Wu, Z. J. Hydroxyl, hydroperoxyl free radicals determination methods in atmosphere and troposphere. *J. Environ. Sci.* **2021**, *99*, 324−335.
(27) Glowacki, D. R.; Goddard, A.; Hemavibool, K.; Malkin, T. L.; Commane, R.; Anderson, F.; Bloss, W. J.; Heard, D. E.; Ingham, T.; Pilling, M. J.; et al. Design of and initial results from a Highly Instrumented Reactor for Atmospheric Chemistry (HIRAC). *Atmospheric Chemistry and Physics* **2007**, *7* (20), 5371−5390.
(28) Winiberg, F. A. F.; Smith, S. C.; Bejan, I.; Brumby, C. A.; Ingham, T.; Malkin, T. L.; Orr, S. C.; Heard, D. E.; Seakins, P. W. Pressure-dependent calibration of the OH and HO_2 channels of a FAGE HOx instrument using the Highly Instrumented Reactor for Atmospheric Chemistry (HIRAC). *Atmos. Meas. Technol.* **2015**, *8* (2), 523−540.
(29) Winiberg, F. A. F.; Dillon, T. J.; Orr, S. C.; Gross, C. B. M.; Bejan, I.; Brumby, C. A.; Evans, M. J.; Smith, S. C.; Heard, D. E.; Seakins, P. W. Direct measurements of OH and other product yields from the HO_2 + $CH_3C(O)O_2$ reaction. *Atmos. Chem. Phys.* **2016**, *16* (6), 4023−4042.
(30) Onel, L.; Brennan, A.; Gianella, M.; Ronnie, G.; Aguila, A. L.; Hancock, G.; Whalley, L.; Seakins, P. W.; Ritchie, G. A. D.; Heard, D. E. An intercomparison of HO_2 measurements by fluorescence assay by gas expansion and cavity ring-down spectroscopy within HIRAC (Highly Instrumented Reactor for Atmospheric Chemistry). *Atmos. Meas. Technol.* **2017**, *10* (12), 4877−4894.
(31) Cantrell, C. A.; Zimmer, A.; Tyndall, G. S. Absorption cross sections for water vapor from 183 to 193 nm (vol 24, pg 2195, 1997). *Geophys. Res. Lett.* **1997**, *24* (21), 2687−2687.
(32) Creasey, D. J.; Heard, D. E.; Lee, J. D. Absorption cross-section measurements of water vapour and oxygen at 185 nm. Implications for the calibration of field instruments to measure OH, HO_2 and RO_2 radicals. *Geophys. Res. Lett.* **2000**, *27* (11), 1651−1654.
(33) Winiberg, F. A. F.Characterisation of FAGE apparatus for HOx detection and application in an environmental chamber, PhD. thesis. University of Leeds, Leeds, UK, 2014.
(34) Maricq, M. M.; Szente, J. J.; Kaiser, E. W.; Shi, J. C. Reaction of chlorine atoms with methylperoxy and ethylperoxy radicals. *J. Phys. Chem.* **1994**, *98* (8), 2083−2089.
(35) Jungkamp, T. P. W.; Kukui, A.; Schindler, R. N. Determination of rate constants and product branching ratios for the reactions of CH_3O_2 and CH_3O with cl atoms at room temperature. *Berichte Der Bunsen-Gesellschaft-Physical Chemistry Chemical Physics* **1995**, *99* (8), 1057−1066.
(36) Atkinson, R.; Baulch, D. L.; Cox, R. A.; Crowley, J. N.; Hampson, R. F.; Hynes, R. G.; Jenkin, M. E.; Rossi, M. J.; Troe, J.; Wallington, T. J. Evaluated kinetic and photochemical data for atmospheric chemistry: Volume IV - gas phase reactions of organic halogen species. *Atmos. Chem. Phys.* **2008**, *8* (15), 4141−4496.
(37) Hochanadel, C. J.; Ogren, P. J.; Ghormley, J. A. Absorption spectrum and reaction kinetics of HO_2 radical in gas-phase. *J. Chem. Phys.* **1972**, *56* (9), 4426.

https://doi.org/10.1021/acs.jpca.2c04968
J. Phys. Chem. A 2022, 126, 7639−7649

(38) Paukert, T. T.; Johnston, H. S. Spectra and kinetics of hydroperoxyl free radical in gas phase. *J. Chem. Phys.* **1972**, *56* (6), 2824−2838.
(39) Moortgat, G.; Veyret, B.; Lesclaux, R. Absorption spectrum and kinetics of reactions of the acetylperoxy radical. *J. Phys. Chem.* **1989**, *93* (6), 2362−2368.
(40) Dusanter, S.; Vimal, D.; Stevens, P. S. Technical note: Measuring tropospheric OH and HO_2 by laser-induced fluorescence at low pressure. A comparison of calibration techniques. *Atmos. Chem. Phys.* **2008**, *8* (2), 321−340.
(41) Schlosser, E.; Brauers, T.; Dorn, H. P.; Fuchs, H.; Haseler, R.; Hofzumahaus, A.; Holland, F.; Wahner, A.; Kanaya, Y.; Kajii, Y.; et al. Technical Note: Formal blind intercomparison of OH measurements: results from the international campaign HOxComp. *Atmospheric Chemistry and Physics* **2009**, *9* (20), 7923−7948.
(42) Fuchs, H.; Dorn, H. P.; Bachner, M.; Bohn, B.; Brauers, T.; Gomm, S.; Hofzumahaus, A.; Holland, F.; Nehr, S.; Rohrer, F.; T.; et al. Comparison of OH concentration measurements by DOAS and LIF during SAPHIR chamber experiments at high OH reactivity and low NO concentration. *Atmos. Meas. Technol.* **2012**, *5* (7), 1611−1626.
(43) Whalley, L. K.; Edwards, P. M.; Furneaux, K. L.; Goddard, A.; Ingham, T.; Evans, M. J.; Stone, D.; Hopkins, J. R.; Jones, C. E.; Karunaharan, A.; et al. Quantifying the magnitude of a missing hydroxyl radical source in a tropical rainforest. *Atmos. Chem. Phys.* **2011**, *11* (14), 7223−7233.
(44) Whalley, L. K.; Furneaux, K. L.; Goddard, A.; Lee, J. D.; Mahajan, A.; Oetjen, H.; Read, K. A.; Kaaden, N.; Carpenter, L. J.; Lewis.; et al. The chemistry of OH and HO_2 radicals in the boundary layer over the tropical Atlantic Ocean. *Atmos. Chem. Phys.* **2010**, *10* (4), 1555−1576.
(45) Whalley, L. K.; Stone, D.; Dunmore, R.; Hamilton, J.; Hopkins, J. R.; Lee, J. D.; Lewis, A. C.; Williams, P.; Kleffmann, J.; Laufs, S.; et al. Understanding in situ ozone production in the summertime through radical observations and modelling studies during the Clean air for London project (ClearfLo). *Atmos. Chem. Phys.* **2018**, *18* (4), 2547−2571.
(46) Monks, P. S.; Carpenter, L. J.; Penkett, S. A.; Ayers, G. P. Night-time peroxy radical chemistry in the remote marine boundary layer over the Southern ocean. *Geophys. Res. Lett.* **1996**, *23* (5), 535−538.

https://doi.org/10.1021/acs.jpca.2c04968
J. Phys. Chem. A 2022, 126, 7639−7649